

Interaction between PAR-3 and the aPKC–PAR-6 complex is indispensable for apical domain development of epithelial cells

Yosuke Horikoshi^{1,*}, Atsushi Suzuki¹, Tomoyuki Yamanaka^{1,‡}, Kazunori Sasaki¹, Keiko Mizuno¹, Hajime Sawada², Shigenobu Yonemura³ and Shigeo Ohno^{1,§}

¹Department of Molecular Biology, Yokohama City University Graduate School of Medical Science, 3-9 Fuku-ura, Kanazawa-ku, Yokohama 236-0004, Japan

²Department of Histology and Cell Biology, Yokohama City University Graduate School of Medical Science, 3-9 Fuku-ura, Kanazawa-ku, Yokohama 236-0004, Japan

³Electron Microscope Laboratory, RIKEN Center for Developmental Biology, 2-2-3 Minatojima-minamimachi, Chuo-ku, Kobe 650-0047, Japan

*Present address: Laboratory of Membrane and Cytoskeleton Dynamics, Institute of Molecular and Cellular Biosciences, The University of Tokyo, 1-1-1 Yayoi, Bunkyo-ku, Tokyo 113-0032, Japan

‡Present address: Laboratory for Structural Neuropathology, RIKEN Brain Sciences Institute, 2-1 Hirosawa, Wako, Saitama 351-198, Japan

§Author for correspondence (e-mail: ohnos@med.yokohama-cu.ac.jp)

Accepted 10 February 2009

Journal of Cell Science 122, 1595–1606 Published by The Company of Biologists 2009
doi:10.1242/jcs.043174

Summary

The evolutionarily conserved polarity proteins PAR-3, atypical protein kinase C (aPKC) and PAR-6 critically regulate the apical membrane development required for epithelial organ development. However, the molecular mechanisms underlying their roles remain to be clarified. We demonstrate that PAR-3 knockdown in MDCK cells retards apical protein delivery to the plasma membrane, and eventually leads to mislocalized apical domain formation at intercellular regions in both two-dimensional and three-dimensional culture systems. The defects in PAR-3 knockdown cells are efficiently rescued by wild-type PAR-3, but not by a point mutant (S827/829A) that lacks the ability to interact with aPKC, indicating that formation of the PAR-3–aPKC–PAR-6 complex is essential for apical membrane development. This is in sharp contrast with tight junction maturation, which does not necessarily depend on the aPKC–PAR-3 interaction, and indicates that the two

fundamental processes essential for epithelial polarity are differentially regulated by these polarity proteins. Importantly, highly depolarized cells accumulate aPKC and PAR-6, but not PAR-3, on apical protein-containing vacuoles, which become targeted to PAR-3-positive primordial cell-cell contact sites during the initial stage of the repolarization process. Therefore, formation of the PAR-3–aPKC–PAR-6 complex might be required for targeting of not only the aPKC–PAR-6 complex but also of apical protein carrier vesicles to primordial junction structures.

Supplementary material available online at
<http://jcs.biologists.org/cgi/content/full/122/10/1595/DC1>

Key words: PAR, aPKC, Epithelial cells, Polarity, Apical domain

Introduction

Epithelial sheets in multicellular organisms form physiological barriers to the external environment (Yeaman et al., 1999). For this purpose, each epithelial cell develops a specific junction structure called the zonula adherens (ZA) that continuously surrounds the apex of the cell. ZA formation is followed by the development of tight junctions (TJs) in mammals or septate junctions in *Drosophila*, which restrict paracellular diffusion of ions and solutes (Knust and Bossinger, 2002). The epithelial cells also segregate their plasma membrane into functionally distinct apical and basolateral membrane domains, which face the external and internal environments of the organism, respectively (Mostov et al., 2003). Studies over the last decade have revealed that the development of these features of epithelial cells, collectively referred to as apicobasal polarity, crucially depends on a set of evolutionarily conserved polarity proteins: PAR-3, atypical protein kinase C (aPKC) and PAR-6 (Macara, 2004; Suzuki and Ohno, 2006).

PAR-3, aPKC and PAR-6 localize to the apical domain of epithelial cells and are concentrated in a subapical region (SAR) above the ZA where mammalian cells develop TJs (Knust and Bossinger, 2002). Accumulating evidence has established that

these polarity proteins are essential for the maturation of epithelial-specific junction structures, such as the ZA and TJs (Macara, 2004; Suzuki and Ohno, 2006). PAR-3, aPKC and PAR-6 have also been shown to play crucial roles in establishing the apical membrane domain. For example, in *Drosophila* blastoderm development, PAR-3 (Baz) and PAR-6 are required for generating and maintaining the apical domain identity (Bilder et al., 2003; Hutterer et al., 2004; Tanentzapf and Tepass, 2003). Targeted disruption of the mouse PAR-3 gene (*Pard3*) impairs apical domain development and lumen formation in epicardial progenitor cells (Hirose et al., 2006). A recent study also provided evidence that aPKC and PAR-6 are involved in apical lumen formation in three-dimensional (3D) cysts of Madin-Darby canine kidney (MDCK) epithelial cells (Martin-Belmonte et al., 2007). Interestingly, studies of *Drosophila* blastoderm development revealed that PAR-3 demarcates the apical membrane domain before completion of the continuous ZA (Bilder et al., 2003; Harris and Peifer, 2004). Furthermore, a recent study demonstrated that cultured mammalian epithelial cells can develop an apical membrane domain without TJs (Adachi et al., 2006). These results suggest that PAR-3, aPKC and PAR-6 differentially regulate apical

domain development and the maturation of epithelia-specific continuous junction structures. However, the underlying molecular mechanisms regulating these two events essential for epithelial polarity remain poorly understood.

Previous biochemical analyses have revealed that PAR-6 forms a stable complex with aPKC (the aPKC–PAR-6 complex), and mediates Rac1- or Cdc42-dependent activation of aPKC (Suzuki et al., 2001; Yamanaka et al., 2001). PAR-3 interacts with the aPKC–PAR-6 complex predominantly via aPKC, and induces the formation of the tripartite PAR-3–aPKC–PAR-6 complex (Izumi et al., 1998; Suzuki et al., 2001). Importantly, accumulating evidence has demonstrated that the formation of the PAR-3–aPKC–PAR-6 complex is dynamically regulated. For example, aPKC phosphorylates Ser827 within the aPKC-binding region of PAR-3 and thereby downregulates its own affinity for PAR-3 (Nagai-Tamai et al., 2002). Rho kinase also disrupts the PAR-3–aPKC interaction by phosphorylating Thr883 of PAR-3, thereby suppressing the activity of the PAR-3–aPKC–PAR-6 complex (Nakayama et al., 2008). The interaction between PAR-3 and the aPKC–PAR-6 complex is also subject to regulation by Lethal giant larvae [Lgl; L(2)gl], which localizes to the basolateral membrane and restricts PAR-3–aPKC–PAR-6 complex activity to the apical membrane (Hutterer et al., 2004). This activity of Lgl is achieved by competing with PAR-3 for binding to the aPKC–PAR-6 complex (Yamanaka et al., 2006; Yamanaka et al., 2003). These results suggest that the interaction between PAR-3 and aPKC is one of the major targets for regulating the activity and localization of the PAR-3–aPKC–PAR-6 complex. The dynamic nature of the PAR-3–aPKC–PAR-6 complex might explain why PAR-3 and the aPKC–PAR-6 complex do not always colocalize in many epithelial cells (Harris and Peifer, 2005; Martin-Belmonte et al., 2007; Nam and Choi, 2003; Suzuki and Ohno, 2006; Vogelmann and Nelson, 2005).

Recently, we demonstrated that increased formation of the PAR-3–aPKC–PAR-6 complex in Lgl knockdown MDCK cells results in severe defects in the apical domain disassembly induced by calcium depletion or type I collagen overlay (Yamanaka et al., 2006). As a result, Lgl knockdown cells fail to form 3D cysts with a central lumen in type I collagen gels, and instead develop abnormal cell aggregates in which the apical proteins are mislocalized to the cell–extracellular matrix interface. These findings indicate that the dynamic regulation of the interaction between PAR-3 and the aPKC–PAR-6 complex is crucial for epithelial tissue morphogenesis, in which the asymmetric membrane domains are dynamically disrupted and regenerated. In the present study, we created PAR-3 knockdown MDCK cells and demonstrate that formation of the PAR-3–aPKC–PAR-6 complex is essential for apical domain development. This is in sharp contrast with recent results showing that PAR-3 can regulate TJ development without any interaction with the aPKC–PAR-6 complex (Chen and Macara, 2005). The present results further suggest that the interaction between PAR-3 and the aPKC–PAR-6 complex might be important for correct targeting of apical protein carrier vesicles to primordial junction structures.

Results

PAR-3 knockdown in MDCK cells induces a delay in apical domain development

Previously, we established a stable MDCK clone (13-32) in which PAR-3 expression was specifically knocked down (Yamanaka et al., 2006). To elucidate the role of PAR-3 in apical domain

development, we analyzed the repolarization process of PAR-3 knockdown cells induced by a calcium switch (CS) (Fig. 1A,B). In addition to the previously reported delay in TJ development (Chen and Macara, 2005), immunostaining of apical marker proteins, such as ezrin and gp135 (podocalyxin), revealed significant impairment of apical domain development in PAR-3 knockdown cells (Fig. 1A,B). Even at 3 hours after the CS, when ezrin and gp135 had completed their polarized localization on the free surface of control cells, they did not show cell surface distributions in most PAR-3 knockdown cells. Instead, PAR-3 knockdown cells segregated these proteins into intracellular vesicle-like compartments that were strongly co-stained with rhodamine-phalloidin (Fig. 1B). Ultrastructural analysis revealed that the inner surfaces of these compartments were rich in microvilli (Fig. 1C), indicating that they corresponded to vacuolar apical compartments (VACs).

VACs are preformed apical membrane structures that are thought to be induced by homotypic fusion of short-lived apical carrier vesicles when plasma membrane delivery is blocked (Vega-Salas et al., 1987). They have been shown to fuse with the plasma membrane in the vicinity of primordial cell–cell junctions upon re-establishment of cell–cell contacts (Vega-Salas et al., 1988). Indeed, VACs were observed in ~50% of control MDCK cells cultured in low-calcium medium for more than 20 hours, and completely disappeared within 5 hours after a CS (Fig. 1D). By contrast, VACs remained in ~25% of PAR-3 knockdown cells even at 5 hours after a CS, although the initial proportions of VAC-containing cells did not differ significantly between control and PAR-3 knockdown cells (Fig. 1D). These results indicate that loss of PAR-3 causes a delay in apical domain development due to retarded VAC exocytosis.

Lack of PAR-3 expression eventually results in intercellular lumen formation

As reported previously (Chen and Macara, 2005), most of the PAR-3 knockdown cells completed TJ reformation within 24 hours after a CS (Fig. 1A). However, we noticed that in addition to the honeycomb pattern of TJs, PAR-3 knockdown cells frequently developed small ring-like TJs containing ZO-1 (Tjp1), occludin and claudin 2 (Fig. 1A, arrowheads; data not shown), which surrounded luminal structures in which the apical proteins and F-actin were concentrated (Fig. 1A,B, arrowheads). In xy images, some luminal structures appeared to be located interiorly. However, analysis of confocal z-stack images with E-cadherin staining revealed that these structures represented intercellular lumens fused with the lateral membrane intruding under the neighboring cells (Fig. 1E,F). Ectopic TJs were formed at the boundary between these intercellular lumens and the lateral membrane independently of the apical TJs. Collectively, these results indicated that PAR-3 knockdown results in mislocalization of the apical domain at cell–cell contact regions. The similar incidences of this apical domain mislocalization (~30%) and the delay in VAC exocytosis (~25%) suggested that these two defects were closely related. In fact, both defects were detected in another PAR-3 knockdown stable MDCK clone (25a) generated using a different targeted sequence, and were restored by overexpression of siRNA-resistant PAR-3 (see Fig. 4B,C; Fig. 5A,B). Importantly, albeit at lower frequency, intercellular lumen formation was even observed in PAR-3 knockdown MDCK cells cultured under normal growth conditions (supplementary material Fig. S1). Therefore, the observed defects in apical domain development were not specific to the cells subjected to a CS, which were forced to induce the formation of easily detectable VACs. These observations are consistent with recent arguments that VAC

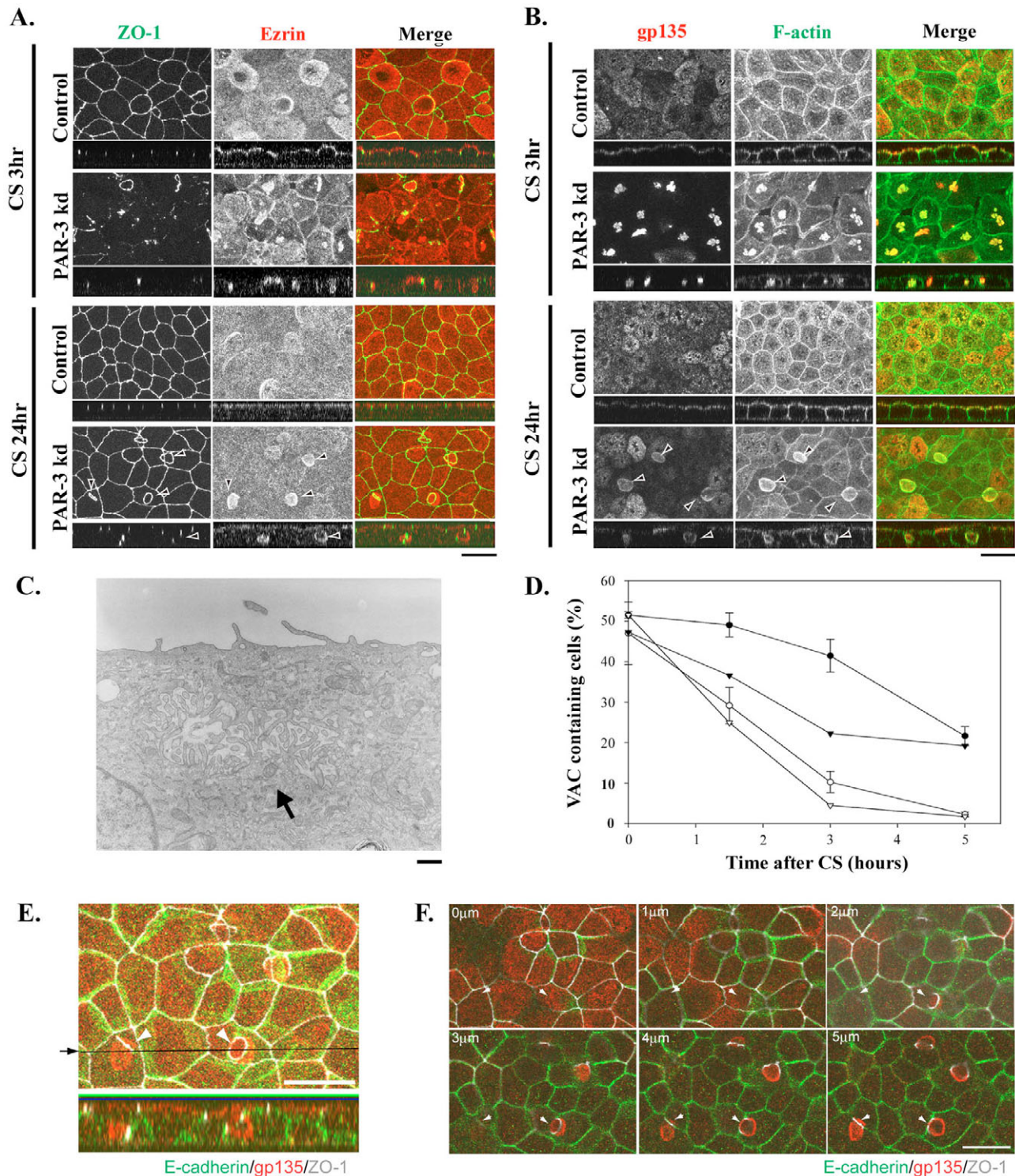


Fig. 1. PAR-3 knockdown retards apical membrane domain development in the early phase of cell polarization. (A,B) Control or PAR-3 knockdown stable MDCK clones (clones 11-10 and 13-32, respectively) were cultured on filter supports and subjected to a calcium switch (CS). At 3 and 24 hours after the CS, the cells were immunostained for ezrin and ZO-1 (A) or gp135 and F-actin (B). Projected views of confocal sections are presented with z-sectional views. Arrowheads indicate intercellular lumens. (C) Transmission electron micrograph of PAR-3 knockdown stable clone (13-32) cells cultured on a filter support and subjected to a CS. At 3 hours after the CS, the cells were fixed and sectioned perpendicularly to the substratum. Arrow indicates vacuolar apical compartments (VACs). (D) Time courses of VAC exocytosis induced by a CS (time 0) were quantified for control (clone 11-10, white circles; clone 1-5, black circles) and PAR-3 knockdown (clone 13-32, black triangles) stable MDCK clones. VACs are identified as large intracellular structures strongly stained for gp135 and F-actin. (E) The data for the PAR-3 knockdown cells shown in the bottom panels in A were supplemented with E-cadherin staining (green) and magnified. The arrow and horizontal black line indicate the position at which the z-sectional view shown at the bottom was reconstituted. Arrowheads indicate intercellular lumens. (F) Original z-stack images of the data in E presented in a gallery from the apical domain to basal domain at 1-μm intervals. Arrowheads indicate intercellular lumens. Scale bars: 20 μm in A,B,E,F; 0.5 μm in C.

formation reflects the normal process of apical domain development, which involves small short-lived vesicles (Lakkaraju and Rodriguez-Boulant, 2007; Mostov and Martin-Belmonte, 2006). Taken together, these results suggest that lack of PAR-3 expression suppresses the plasma membrane fusion of apical membrane carrier vesicles and eventually causes mislocalization of the apical domain within the intercellular regions.

PAR-3 knockdown results in the formation of multiple-lumen cysts in collagen gels

Next, we examined the effects of PAR-3 knockdown on MDCK cystogenesis, which was observed when cells were cultured in type I collagen gels (Fig. 2). In these experiments, we initially used PAR-3 knockdown cells (#1 and #2) established using an autonomous replicative shRNA vector, pEB6-SUPER (see

Materials and Methods) (supplementary material Fig. S2) (Suzuki et al., 2004; Yamanaka et al., 2006). As previously reported (O'Brien et al., 2002), control MDCK cells formed 3D cysts consisting of single polarized monolayers enclosing a central lumen (Fig. 2A,B). In these cysts, immunofluorescence signals for F-actin and gp135 were enriched in the membrane facing the central lumen. By contrast, PAR-3 knockdown cells frequently developed abnormal cysts with multiple lumens that were positive for gp135 and F-actin (Fig. 2A-C). Careful inspection of serial optical sections of these multiple-lumen cysts revealed that every PAR-3 knockdown cell exhibited contact with one of the lumens (Fig. 3A). Furthermore, in these PAR-3 knockdown cysts, E-cadherin was excluded from the luminal surfaces (Fig. 2A). ZO-1 and occludin were identified in every cell at the tips of cell-cell contacts adjacent to the lumens (Fig. 2A; data not shown). In

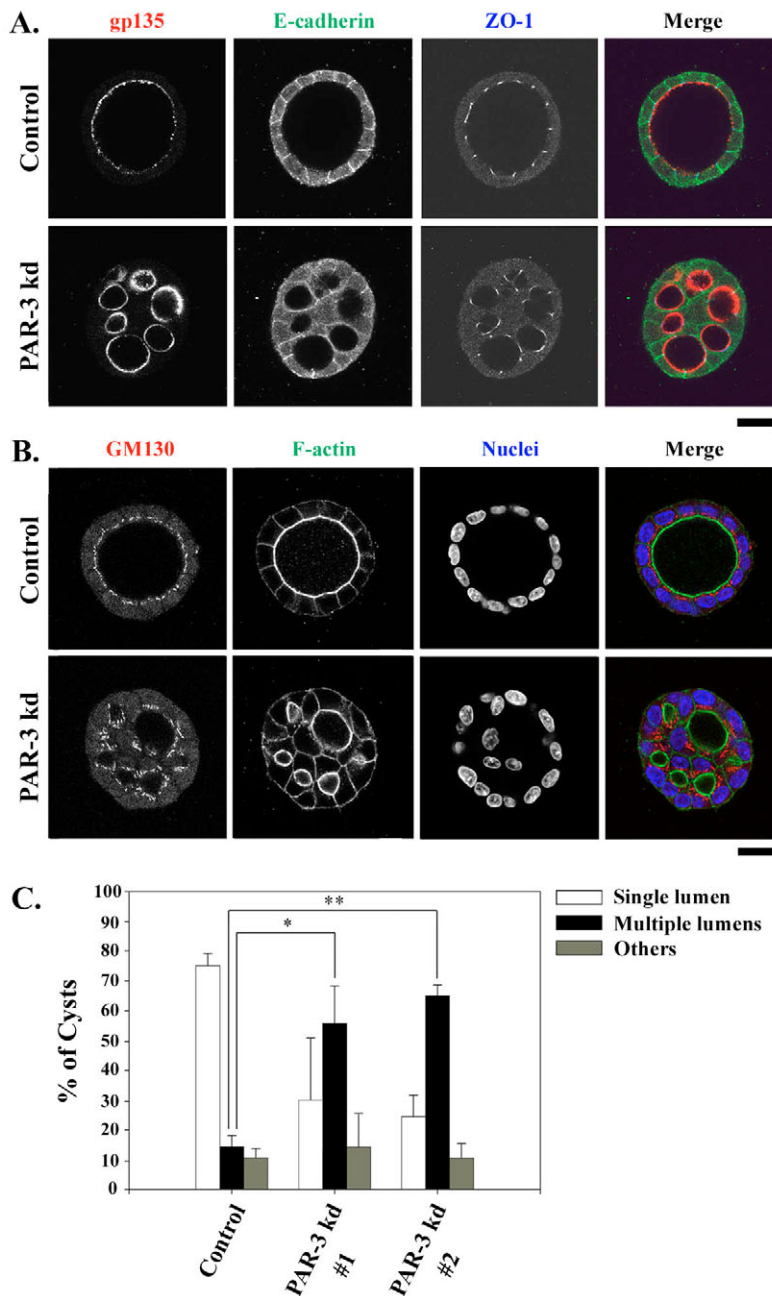


Fig. 2. PAR-3 knockdown MDCK cells fail to form normal cysts with an integrated single lumen. (A,B) Control or PAR-3 knockdown (2) cells were embedded in type I collagen gels and cultured for 7 days. The resulting cysts were fixed and immunostained for gp135, E-cadherin and ZO-1 (A) or GM130, F-actin and nuclei (TOPRO3) (B) as indicated. Confocal single sections are presented. Note that PAR-3 knockdown cells are polarized, but the apical domain of each cell is not integrated as a single lumen. (C) Cysts containing single or multiple lumens were counted for control and PAR-3 knockdown (#1 and #2) cells. Amorphous-shaped cysts with no lumen were categorized into 'others'. **P* < 0.001, ***P* < 0.05 versus control cells by Student's *t*-test. The error bars indicate the s.d. (*n*=3). Scale bars: 20 μm.

addition, the Golgi marker GM130 (Golga2) was asymmetrically distributed above the luminal side of the nuclei (Fig. 2B). These results indicate that in individual PAR-3 knockdown cells the apicobasal polarity was established at least partially, but the apical domain of each cell was not properly integrated. Again, this defect was attributable to reduced expression of PAR-3 because two different siRNA sequences gave rise to similar results (Fig. 2C). Moreover, a PAR-3 knockdown stable MDCK clone (25a) showed similar defects in cystogenesis, which could be restored by overexpression of siRNA-resistant wild-type PAR-3 (see Fig. 4D). To gain further insight into the defect in cystogenesis of PAR-3 knockdown cells, we analyzed the time course of cyst formation. Control MDCK cells formed a single central lumen, even in three- to four-cell cysts that were predominantly observed at 2 days after cell embedding (Fig. 3B). This finding is consistent with previous results showing that the establishment and coordination of apicobasal polarity in each cell occur at a very early stage of cystogenesis (Martin-Belmonte et al., 2007; Straight et al., 2004). Importantly, separated lumens were frequently observed at cell-cell contact regions at the three- to four-cell stage of PAR-3 knockdown cysts (Fig. 3B,C). Furthermore, we sometimes detected large vacuolar structures rich in gp135 and F-actin, but not β -catenin, in both control and PAR-3 RNAi cells at the very

early stage of cystogenesis (Fig. 3C). These results suggest that the abnormal cystogenesis of PAR-3 knockdown cells is caused by mislocalization of the apical membrane, as observed in two-dimensional (2D) monolayers.

The interaction between PAR-3 and aPKC is required for normal apical domain development

Recently, aPKC binding was shown to be dispensable for PAR-3 to rescue TJ formation in PAR-3 knockdown cells (Chen and Macara, 2005). The evidence provided revealed that interaction with the Rac exchange factor Tiam1 is important for PAR-3 to control TJ assembly. To examine whether the interaction between PAR-3 and aPKC is also dispensable for apical domain development, we examined a PAR-3 point mutant lacking aPKC-binding activity (PAR-3 S827/829A) (Fig. 4A; supplementary material Fig. S3) for its ability to restore normal apical domain development in PAR-3 knockdown cells (Nagai-Tamai et al., 2002). Overexpression of RNAi-resistant wild-type PAR-3 significantly restored both TJ formation and apical domain development in PAR-3 knockdown cells (Fig. 4B,C). Furthermore, consistent with the results of Chen and Macara (Chen and Macara, 2005), PAR-3 S827/829A restored TJ formation to a level comparable to wild-type PAR-3 at 3 hours after a CS (Fig. 4B,C). However, PAR-3 S827/829A showed

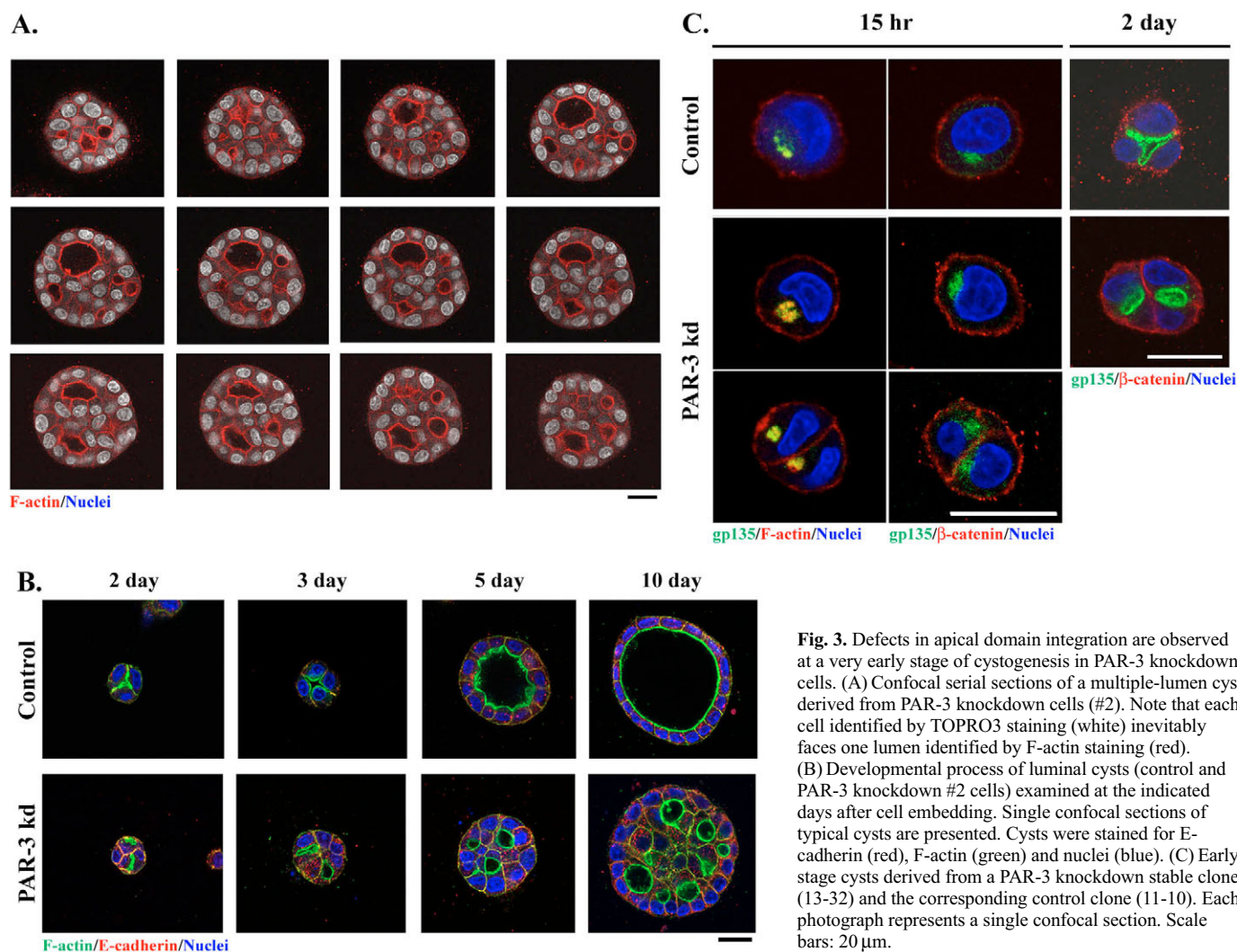


Fig. 3. Defects in apical domain integration are observed at a very early stage of cystogenesis in PAR-3 knockdown cells. (A) Confocal serial sections of a multiple-lumen cyst derived from PAR-3 knockdown cells (#2). Note that each cell identified by TOPRO3 staining (white) inevitably faces one lumen identified by F-actin staining (red). (B) Developmental process of luminal cysts (control and PAR-3 knockdown #2 cells) examined at the indicated days after cell embedding. Single confocal sections of typical cysts are presented. Cysts were stained for E-cadherin (red), F-actin (green) and nuclei (blue). (C) Early-stage cysts derived from a PAR-3 knockdown stable clone (13-32) and the corresponding control clone (11-10). Each photograph represents a single confocal section. Scale bars: 20 μ m.

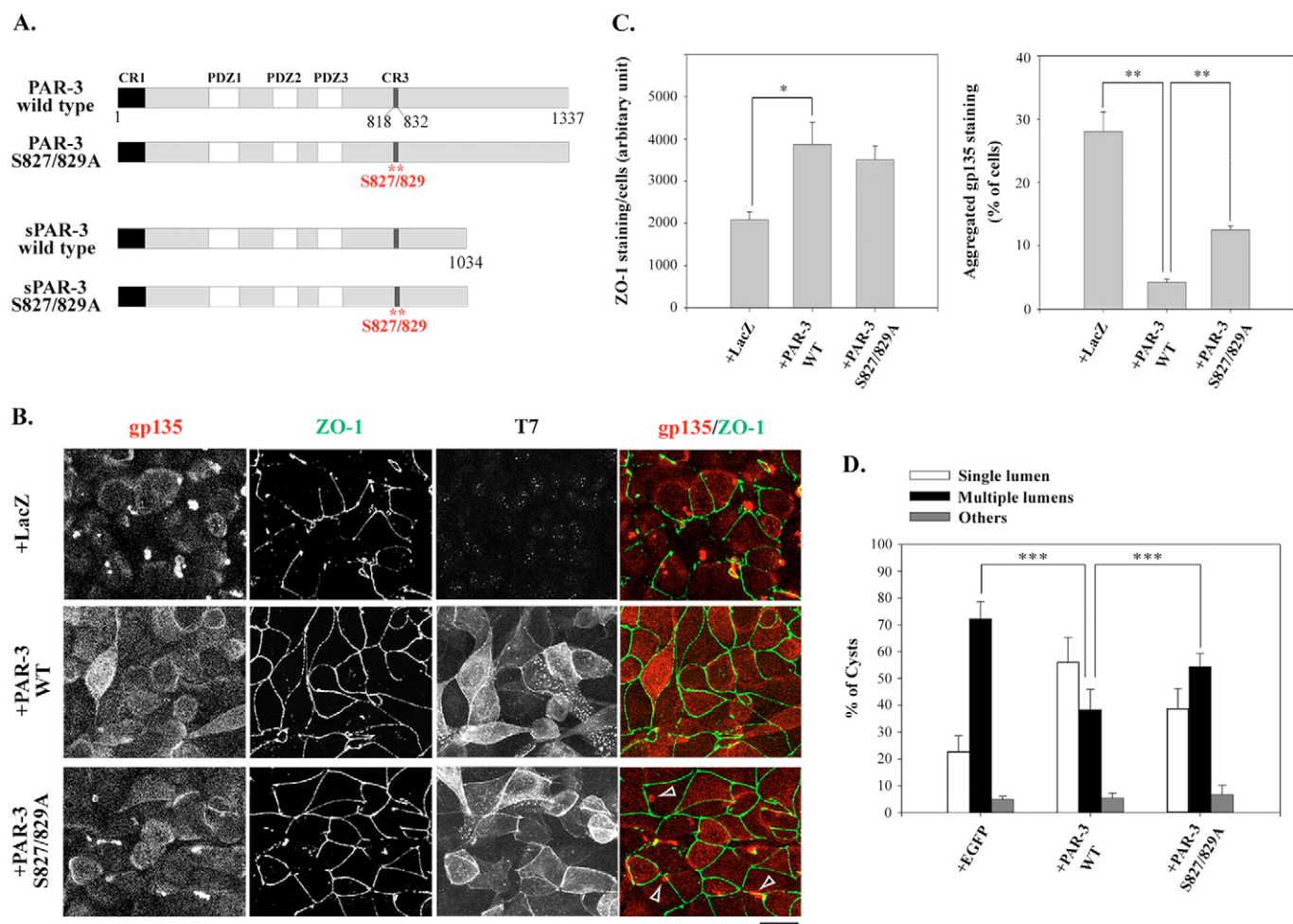


Fig. 4. PAR-3 S827/829A restores VAC exocytosis in PAR-3 knockdown cells less efficiently than wild-type PAR-3. (A) The PAR-3 isoforms and their S827/829A point mutants used in this study. CR3 is the aPKC-binding region. Red asterisks indicate the positions of mutated serine residues. (B) PAR-3 knockdown stable clone (25a) cells cultured on filter supports were infected with adenovirus expression vectors encoding β -galactosidase, T7-tagged wild-type PAR-3 or T7-tagged PAR-3 S827/829A. After 2 days, the cells were subjected to a CS. At 3 hours after the CS, the cells were immunostained for the indicated components to examine both apical domain re-establishment and junction reassembly. Projected views of confocal sections are presented. Equal expression levels of wild-type PAR-3 and its mutant are confirmed by the immunostaining as well as by western blotting (supplementary material Fig. S3) with an anti-T7 antibody. Arrowheads indicate VACs associated with continuous ZO-1 staining. Scale bars: 20 μ m. (C) Quantification of the results shown in B. (Left) The average fluorescence intensity of ZO-1 staining (density) at cell-cell borders per cell was quantified as described in the Materials and Methods. Bars indicate the mean \pm s.d. of four independent experiments. * P <0.01. The difference between wild-type and mutant PAR-3-expressing cells is not significant (P =0.38). (Right) The ratios of VAC-containing cells were estimated for cells expressing the indicated exogenous proteins. Bars indicate the mean \pm s.d. of four independent experiments. ** P <0.001. (D) PAR-3 knockdown stable clone (25a) cells stably expressing EGFP, T7-tagged wild-type PAR-3 or T7-tagged PAR-3 S827/829A under the control of tetracycline-inducible transactivation were established using the pOSTet14 expression vector. Cysts of each cell type were analyzed as described in the legend for Fig. 2. Expression of the exogenous proteins was induced by adding doxycycline (200 ng/ml) to the culture medium, and equal expression levels of wild-type PAR-3 and its mutant were confirmed by western blotting with an anti-PAR-3 antibody (supplementary material Fig. S3). Data represent the mean \pm s.d. of three independent experiments. *** P <0.05.

weaker activity for restoring the delay in VAC exocytosis than wild-type PAR-3. In contrast to wild-type PAR-3-expressing cells, PAR-3 S827/829A-expressing cells frequently showed VAC-like gp135 aggregates within the cells in the vicinity of continuous TJs (Fig. 4B, arrowheads; Fig. 4C). Since this mutant did not induce any defects in apical domain development when overexpressed in wild-type MDCK cells (supplementary material Fig. S4), the above phenotypes were not due to unknown gain-of-abnormal-function by PAR-3 S827/829A, but were caused by its lower activity being insufficient to replace normal PAR-3 function. We also observed a lower rescue activity of PAR-3 S827/829A for 3D cystogenesis. As shown in Fig. 4D, wild-type PAR-3 significantly restored normal cyst formation in PAR-3 knockdown cells, whereas PAR-3

S827/829A exhibited lower activity than wild-type PAR-3 (56.1% versus 38.8%; n =3, P <0.05). Interestingly, the residual rescue activity of PAR-3 S827/829A for apical domain development was completely abolished when the short isoform of PAR-3 (sPAR-3) (Lin et al., 2000), which lacks the C-terminal region, was examined. As shown in Fig. 5, wild-type sPAR-3 still exhibited substantial effects in restoring normal apical domain development in PAR-3 knockdown cells in both 2D (Fig. 5A,B) and 3D (Fig. 5C,D) culture systems. However, sPAR-3 S827/829A did not show any rescue activity in either culture system. These results indicate that the interaction between PAR-3 and aPKC is essential for normal apical domain development in MDCK cells, and that the C-terminal region of PAR-3 might also exert a redundant function independent of

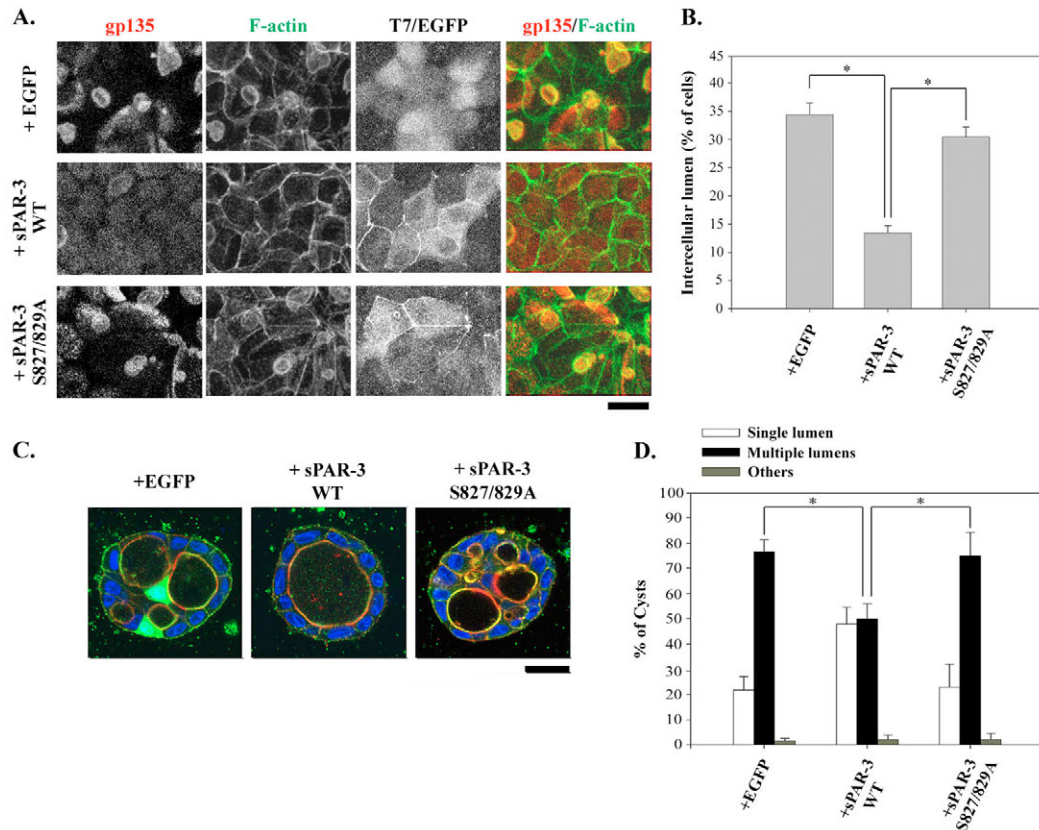


Fig. 5. sPAR-3 S827/829A cannot restore correct apical domain development in PAR-3 knockdown cells. (A) PAR-3 knockdown stable clone (25a) cells stably expressing EGFP, T7-tagged wild-type sPAR-3 or T7-tagged sPAR-3 S827/829A under the control of tetracycline-inducible transactivation were cultured on filter supports for 2 days in the presence of doxycycline (20 ng/ml). The cells were then subjected to a CS. At 20 hours after the CS, the cells were fixed and triply stained for gp135 (red in the merged images), tag (EGFP or T7) and F-actin (green in the merged images). Projected views of confocal sections are presented. Note that PAR-3 knockdown cells expressing wild-type sPAR-3 do not develop lateral lumens, whereas those expressing sPAR-3 S827/829A retain extensive lateral lumens. (B) Quantification of the results in A. The ratios of cells exhibiting intercellular lumens on their lateral membrane were estimated for cells expressing the individual exogenous proteins. The data represent the mean \pm s.d. of three independent experiments. $*P < 0.001$. (C) Cysts derived from PAR-3 knockdown stable clone (25a) cells stably overexpressing EGFP, T7-tagged wild-type sPAR-3 or T7-tagged sPAR-3 S827/829A were stained for EGFP or T7 (green), F-actin (red) and nuclei (blue). Each photograph represents a single confocal section. Expression of the exogenous proteins was induced by adding doxycycline (20 ng/ml) to the culture medium. (D) Quantification of the results in C. The ratios of cysts exhibiting multiple lumens were estimated for cysts expressing the individual exogenous proteins. The rescue efficiencies were quantified as described in the legend for Fig. 2. Data represent the mean \pm s.d. of five independent experiments. $*P < 0.001$. Scale bars: 20 μ m.

aPKC, probably by interacting with other effective proteins such as Tiam1 or KIF3 (Chen and Macara, 2005; Nishimura et al., 2004; Nishimura et al., 2005). Since the interaction between PAR-3 and aPKC provides an essential linkage between PAR-3 and the aPKC–PAR-6 complex (Nakayama et al., 2008; Suzuki et al., 2001), the above results imply that the formation of the PAR-3–aPKC–PAR-6 ternary complex is indispensable for apical domain development.

Formation of the PAR-3–aPKC–PAR-6 complex and aPKC kinase activity are required for normal apical domain development

To further confirm the above conclusion, we examined the effects of overexpression of the mammalian homolog of Lgl (mLgl2). Lgl has been shown to inhibit the formation and function of the PAR-3–aPKC–PAR-6 ternary complex by competing with PAR-3 for binding to the aPKC–PAR-6 complex (Yamanaka et al., 2006; Yamanaka et al., 2003). Overexpression of mLgl2 strongly induced the formation of abnormal lumens in 2D monolayers as well as in 3D cysts (Fig. 6A,B; supplementary material Fig. S5). Furthermore,

overexpression of wild-type PAR-6 β , but not its point mutant PAR-6 β M235W (MW), which lacks the Lgl-binding activity (Yamanaka et al., 2003), also resulted in a marked increase in the number of multiple-lumen cysts (Fig. 6C; supplementary material Fig. S5). Since PAR-6 β overexpression preferentially promotes the formation of the Lgl–aPKC–PAR-6 complex (Yamanaka et al., 2003), these results support the notion that the PAR-3–aPKC–PAR-6 ternary complex is indispensable for normal apical domain development.

Recently, depletion of one of the possible apical domain determinants, namely PTEN, Anx2 or Cdc42, in MDCK cells was shown to result in abnormal cyst formation with multiple intracellular and intercellular small lumens (Martin-Belmonte et al., 2007). Furthermore, these authors reported that treatment of MDCK cysts with an aPKC inhibitor (pseudosubstrate of aPKC ζ) induced similar defects in cystogenesis. Here, we observed that overexpression of a dominant-negative mutant of aPKC λ (aPKC λ KN) resulted in the formation of multiple-lumen cysts (Fig. 6B,C; supplementary material Fig. S5), as observed in PAR-3 knockdown cells. In addition, aPKC λ KN overexpression and aPKC λ knockdown caused a delay in VAC exocytosis and intercellular

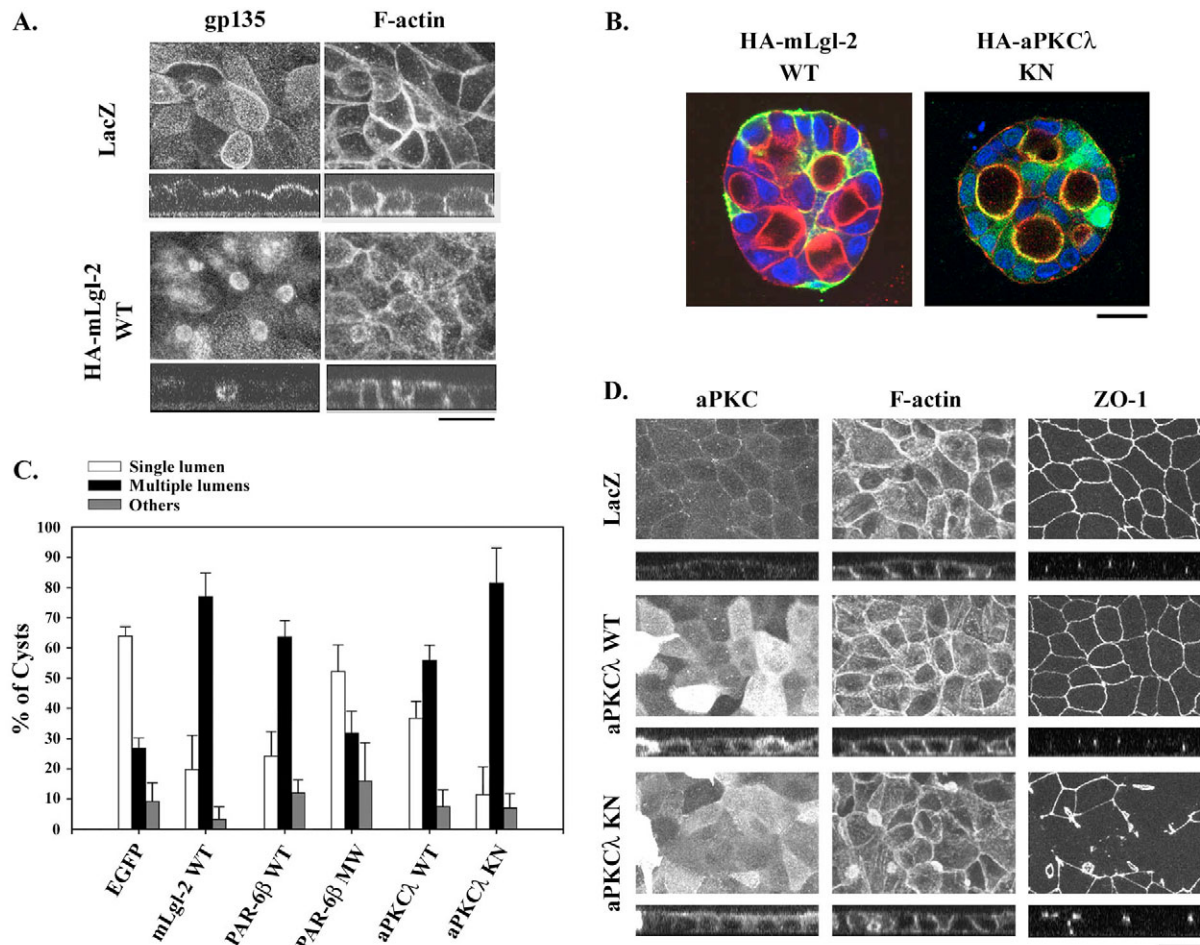


Fig. 6. Formation of the PAR-3-aPKC-PAR-6 complex and aPKC kinase activity are essential for normal apical domain development. (A) MDCK cells cultured on filter supports were infected with adenovirus expression vectors encoding HA-mLgl2. After 2 days, the cells were subjected to a CS. At 10 hours after the CS, the cells were immunostained for F-actin and gp135. Projected views of confocal sections are presented with z-sectional views. (B) Cysts derived from MDCK cells overexpressing HA-mLgl2 or HA-aPKCλ KN were stained for F-actin (red), HA tag (green) and nuclei (blue). (C) Quantification of the effects of HA-mLgl2, HA-aPKCλ WT, HA-aPKCλ KN, T7-PAR-6β WT and T7-PAR-6β M235W (MW) overexpression on cyst formation. The ratios of cysts exhibiting multiple lumens were estimated for cysts expressing the individual exogenous proteins. Bars indicate the mean \pm s.d. of three to five independent experiments. (D) Overexpression of a dominant-negative mutant of aPKCλ (aPKCλ KN), but not wild-type aPKCλ (aPKCλ WT), induces the formation of lateral lumens in 2D-cultured MDCK cells. MDCK cells cultured on filter supports were infected with adenovirus expression vectors encoding the indicated proteins. After 2 days the cells were subjected to a CS. At 10 hours after the CS, the cells were immunostained for aPKC, F-actin and ZO-1. Single confocal sections are presented with z-sectional views. Scale bars: 20 μ m.

lumen formation in 2D monolayers (Fig. 6D; data not shown). These results confirm that aPKC and its kinase activity are required for correct apical domain development. Furthermore, they suggest that the defects in apical domain development caused by PAR-3 knockdown are similar to those induced by loss-of-function of PTEN, Anx2, Cdc42 or aPKC. Interestingly, albeit less significantly, overexpression of wild-type aPKCλ (aPKCλ WT) disturbed apical domain development in 3D cysts but not in 2D monolayers (Fig. 6C). These findings are consistent with the fact that 3D cystogenesis is more sensitive to disturbance of polarity signals than are 2D monolayers (Hurd et al., 2003a; O'Brien et al., 2001), and suggest that strict regulation of the aPKC kinase activity is essential for correct apical domain development.

VACs accumulate aPKC and PAR-6, but not PAR-3, and are targeted to the initial cell-cell contact sites positive for PAR-3. Finally, we re-examined the localization of PAR-3, aPKC and PAR-6 in repolarizing MDCK cells. In these analyses, we used

an anti-PAR-6β antibody that we generated previously (Yamanaka et al., 2003). In western blot analyses, this antibody detected a single band of 50 kDa in MDCK cell extracts (Yamanaka et al., 2003), and did not show any cross-reactivities with PAR-6α and PAR-6γ (supplementary material Fig. S6). In immunofluorescence analyses of polarized MDCK cells, the antibody stained the apical domain and apical junctional complex, as reported previously (Yamanaka et al., 2003). All signals detected in both analyses were significantly reduced in two independent heterogeneous RNAi-stable cells expressing different shRNA sequences for PAR-6β (supplementary material Fig. S6), indicating that the antibody specifically recognizes the endogenous PAR-6β protein.

In cells that are incompletely depolarized in low-calcium medium, aPKC and PAR-6β remain localized to the plasma membrane (Yamanaka et al., 2003). However, when cells were subjected to prolonged incubation (for more than 20 hours) in low-calcium medium and forced to develop VACs, the membrane

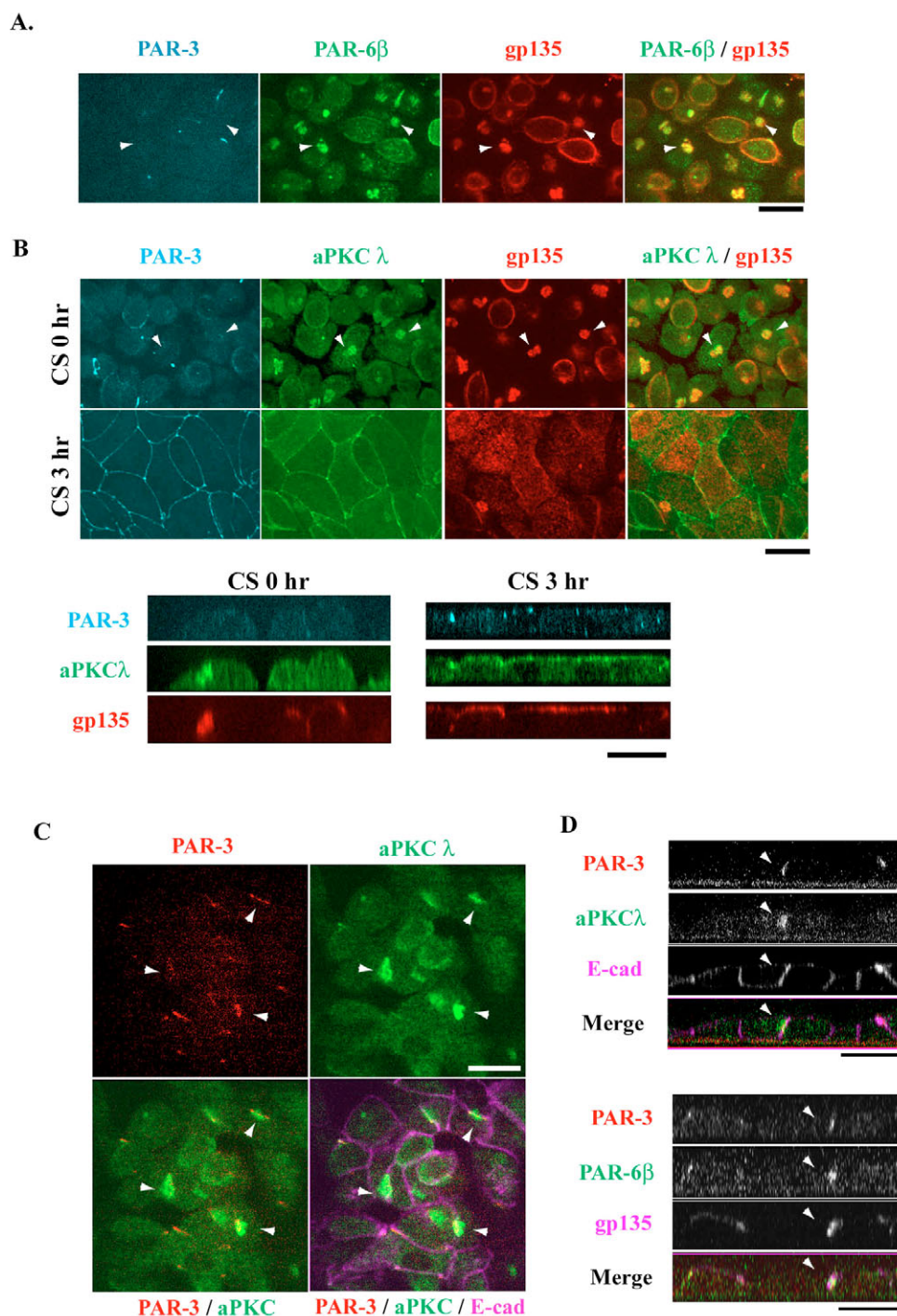


Fig. 7. aPKC and PAR-6, but not PAR-3, accumulate in VACs in extensively depolarized MDCK cells and are targeted to primordial junctions where PAR-3 is concentrated. (A) Control stable clone (11-10) cells cultured on filter supports were depolarized by prolonged incubation (for more than 20 hours) in low-calcium medium, and then immunostained for PAR-6 β , PAR-3 and gp135. Projected views of confocal sections are presented. Arrowheads in all panels indicate the positions of VACs. (B) Cells prepared as in A and those subjected to a CS for 3 hours were immunostained for aPKC, PAR-3 and gp135. The anti-aPKC antibody used (Santa Cruz Biotechnology C20) detects both paralogs of mammalian aPKC (λ and ζ). Projected views of confocal sections are presented with z-sectional views. (C) PAR-3 knockdown stable clone (13-32) cells extensively depolarized in low-calcium medium were subjected to a CS. At 3 hours after the CS, the cells were immunostained for PAR-3, aPKC and E-cadherin. Single confocal sections at the apical side are presented. (D) z-sectional views of cells prepared similarly to in C and immunostained for PAR-3, aPKC and E-cadherin (top) or PAR-3, PAR-6 β and gp135 (bottom). Scale bars: 20 μ m.

localization of aPKC and PAR-6 β almost disappeared and they accumulated on VACs (Fig. 7A,B, arrowheads). Their association with VACs was also confirmed by immunoelectron microscopy (supplementary material Fig. S7; data not shown). Interestingly, PAR-3 was not detected on VACs (Fig. 7A,B), suggesting that the aPKC–PAR-6 complex on VACs was in a form lacking the PAR-3 association. Upon calcium repletion, aPKC and PAR-6 β on VACs were targeted to the plasma membrane, and eventually became distributed on the apical membrane with a concentration at TJs (Fig. 7B). In wild-type MDCK cells, it was difficult to detect the intermediate states of VAC exocytosis,

which proceeded rapidly and heterogeneously. However, we frequently detected the intermediate states of VAC exocytosis in PAR-3 knockdown MDCK cells, in which VACs containing aPKC or PAR-6 β were associated with the plasma membrane (Fig. 7C,D, arrowheads). In most cases, these intermediate states were observed at cell-cell contact regions, where trace amounts of PAR-3 accumulated (Fig. 7C,D, arrowheads). These results are consistent with the notion that the interaction between PAR-3 and the aPKC–PAR-6 complex is involved in cell surface targeting of VACs in the vicinity of primordial cell-cell junctions.

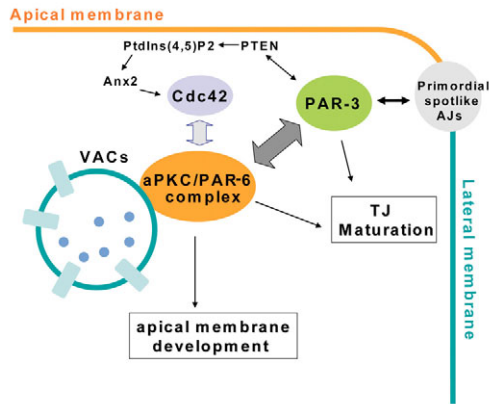


Fig. 8. A model for the mechanism by which aPKC, PAR-6 and PAR-3 regulate apical domain development. See Discussion for details.

Discussion

In the present study, we have demonstrated that PAR-3 knockdown results in a delay of VAC exocytosis and leads eventually to mislocalization of the apical membrane in both 2D monolayers and 3D cysts of MDCK cells. VACs were originally defined in MDCK cells cultured under non-physiological conditions that prevented the formation of cell-cell contacts (Vega-Salas et al., 1987). However, similar intracellular vacuoles have been described under normal culture conditions not only *in vitro* (Bayless and Davis, 2002; Folkman and Haudenschild, 1980) but also *in vivo* (Kamei et al., 2006). These observations suggest that the formation of easily detected VACs represents the normal process of lumen formation, in which smaller short-lived vacuoles are used to build the luminal surface of epithelial cells (Lakkaraju and Rodriguez-Boulant, 2007; Mostov and Martin-Belmonte, 2006). Here, we observed that aPKC and PAR-6, but not PAR-3, accumulated on VACs and were targeted to the PAR-3-containing regions in cell-cell contacts. Together with the finding that the PAR-3–aPKC interaction is indispensable for apical domain development, these results raise the intriguing possibility that PAR-3 provides a landmark for plasma membrane fusion of VACs on which the aPKC–PAR-6 complex is localized (Fig. 8). This idea is consistent with previous observations that PAR-3 localizes to primordial spot-like adherens junctions (AJs) earlier than aPKC and PAR-6 (Harris and Peifer, 2004; Harris and Peifer, 2005; Suzuki et al., 2002) and that an apical membrane protein, aminopeptidase, reappears at regions of cell-cell contacts when subjected to antibody-induced endocytosis (Louvard, 1980). Considering that basolateral membrane proteins have also been demonstrated to be targeted to sites of cell-cell adhesion where the Sec6/8 complex is localized (Yeaman et al., 1999), the present results might imply that the primordial cell-cell contact regions are the active membrane fusion sites for both apical and basolateral membrane development. The interaction between PAR-3 and the aPKC–PAR-6 complex might contribute towards specific facilitation of apical membrane fusions at this region.

Although PAR-3, aPKC and PAR-6 can form a ternary complex, accumulating evidence has revealed that PAR-3 and the aPKC–PAR-6 complex do not always colocalize in epithelial cells (Harris and Peifer, 2005; Martin-Belmonte et al., 2007; Nam and Choi, 2003; Vogelmann and Nelson, 2005). However, if we consider the dynamic nature of the interaction between PAR-3 and aPKC (Nagai-Tamai et al., 2002; Nakayama et al., 2008; Yamanaka et al.,

2003), the distinct localization of PAR-3 as compared with aPKC and PAR-6 does not necessarily contradict the idea that the formation of the PAR-3–aPKC–PAR-6 complex is required for apical domain development. The aPKC–PAR-6 complex might be initially recruited to the plasma membrane through the interaction with PAR-3, but then immediately dissociates from PAR-3 and moves onto other apical membrane-anchoring factors such as Cdc42 or the Crumbs/Pals complexes (Hurd et al., 2003b; Hutterer et al., 2004; Martin-Belmonte et al., 2007; Nam and Choi, 2003). In fact, although Cdc42 depletion was shown to be sufficient for inhibiting the apical membrane localization of aPKC in MDCK cysts (Martin-Belmonte et al., 2007), PAR-3 was found to be required for Cdc42-dependent apical localization of the aPKC–PAR-6 complex in *Drosophila* neuroblasts (Atwood et al., 2007). Furthermore, a study in *Caenorhabditis elegans* embryos revealed that the CDC-42 interaction with PAR-6 is not required for the initial establishment of asymmetry, but is required for maximal cortical accumulation of PAR-6 and the maintenance of asymmetry (Aceto et al., 2006). Interestingly, we previously observed that Lgl knockdown simultaneously enhances the formation of the PAR-3–aPKC–PAR-6 complex and the interaction between PAR-6 and Cdc42 (Yamanaka et al., 2006). Therefore, it is highly plausible that PAR-3 and Cdc42 cooperatively function for membrane targeting of the aPKC–PAR-6 complex. Recently, Cdc42 was shown to be recruited and activated at the apical membrane by the PTEN–PtdIns(4,5)P₂–Anx2 pathway during apical domain development in MDCK cystogenesis (Martin-Belmonte et al., 2007). Considering that PAR-3 was also demonstrated to interact with PTEN (Wu et al., 2007), our results also raise the possibility that the direct interaction between PAR-3 and the aPKC–PAR-6 complex transiently, but efficiently, concentrates the signaling components required for apical domain development, such as PTEN, PtdIns(4,5)P₂, Anx2 and Cdc42, in the vicinity of the primordial cell-cell junctions (Fig. 8).

Despite the significant retardation of VAC exocytosis, PAR-3-depleted MDCK cells eventually exhibited apical domain development, probably owing to residual PAR-3 activity. However, PAR-3 knockdown cells showed other defects in apical domain development at this stage because they exhibited mislocalization of the apical domain at cell-cell contact regions instead of localization at the free surface. This observation raises the question of why the delay in VAC exocytosis led to such mislocalization of the apical membrane domain. In this respect, it is noteworthy that VACs fuse with the plasma membrane below the primordial junctions and transiently induce intercellular lumens (Vega-Salas et al., 1988). The apical membrane components in VACs subsequently move towards their final destination on the free surface. This indicates a possibility that columnar epithelial cells strictly coordinate the spatiotemporal relationship between TJ maturation and VAC exocytosis to avoid trapping the apical components below TJs. Thus, the delay in VAC exocytosis might perturb this putative coordination between VAC exocytosis and TJ maturation, and consequently induces mislocalization of the apical membrane (see below).

Recent studies have demonstrated that PAR-3 regulates TJ formation without any interactions with aPKC and PAR-6 (Chen and Macara, 2005). Since aPKC and its kinase activity are also indispensable for TJ development (Suzuki et al., 2001), these results indicate that both PAR-3 and aPKC are independently required for TJ development (Fig. 8). However, these findings are in sharp contrast to the present results showing that apical domain development depends on a direct interaction between PAR-3 and the aPKC–PAR-

6 complex. Indeed, PAR-3 S827/829A, a PAR-3 point mutant incapable of binding to aPKC, restored VAC exocytosis less efficiently than it did TJ development in PAR-3 knockdown cells. As a result, the cells frequently exhibited normal TJ formation without completion of apical domain development. These results indicate that two of the essential events for epithelial polarity establishment, namely apical domain development and TJ maturation, are differentially regulated by PAR-3, aPKC and PAR-6 (Fig. 8). Importantly, we previously observed that overexpression of another PAR-3 mutant (PAR-3 S827A), which is unable to dissociate from aPKC, inhibits TJ development (Nagai-Tamai et al., 2002). This observation appears to suggest that dissociation of PAR-3 from the aPKC-PAR-6 complex is required for TJ maturation. In combination with the present findings that aPKC and PAR-6 accumulated on VACs, these results raise the intriguing possibility that the dynamic nature of the interaction between PAR-3 and the aPKC-PAR-6 complex provides the molecular basis for the sophisticated coordination between VAC exocytosis and TJ maturation discussed above. Specifically, the aPKC-PAR-3 interaction occurs when VACs are targeted to the primordial junctions and might transiently suppress PAR-3 activity for TJ development. After the apical membrane components from VACs move toward the apical free surface, aPKC liberates PAR-3 by phosphorylating S827, thereby allowing it to function again for TJ development (Hirose et al., 2002).

In this study, we have revealed indispensable roles for the interaction between PAR-3 and the aPKC-PAR-6 complex in apical domain development. Furthermore, we have demonstrated that apical domain development and TJ maturation are differentially regulated by these polarity proteins. The present results provide important insight into how these polarity proteins regulate the development of epithelial polarity. Future studies will reveal in more detail the mechanisms by which these polarity proteins cooperatively promote the complex but sophisticated process of epithelial polarization, including cytoskeletal organization, junction development and asymmetric membrane development.

Materials and Methods

Expression vectors

The following cDNAs have been described previously: T7-tagged mouse PAR-3 isoforms (Mizuno et al., 2003) and its point mutant S827/829A (Nagai-Tamai et al., 2002); HA-tagged mlg2, HA-tagged mouse wild-type aPKC λ and its kinase-deficient mutant (aPKC KN: K273E), T7-tagged human PAR-6 β and its point mutant PAR-6 β (M235W) (Yamanaka et al., 2003). These cDNAs were subcloned into the Epstein-Barr virus (EBV)-based expression vector pEB6-CAG, or its derivative pOSTet14, which can autonomously replicate in MDCK cells (Mishima et al., 2004; Suzuki et al., 2004). Adenovirus expression vectors encoding β -galactosidase or the long isoform of PAR-3 were described previously (Mishima et al., 2002). An adenovirus expression vector encoding the long isoform of PAR-3 S827/829A was newly generated, as described previously (Suzuki et al., 2001), using pAxCawt (TaKaRa).

Antibodies

Anti-PAR-3 polyclonal antibodies (pAbs) were generated in rats or rabbits using the CR3 domain (amino acids 712-936) of rat PAR-3 fused with GST (Izumi et al., 1998; Suzuki et al., 2004). Anti-PAR-6 pAb was generated in rabbit using the C-terminal 14 amino acids as antigen (Yamanaka et al., 2003). An anti-gp135 mouse monoclonal antibody (mAb) (3F2) was a generous gift from Dr J. D. Nelson (Stanford University, CA, USA). All other antibodies were purchased from commercial sources as follows: anti-ZO-1 rat mAb (Chemicon); anti-ZO-1 mouse mAb (Zymed); anti-E-cadherin, anti-aPKC ζ and anti-GM130 mouse mAbs (BD Transduction Laboratories); anti-PAR-3 pAb (Upstate Biotechnology); anti-aPKC ζ pAb (C20) and T7 (omni probe) pAb (Santa Cruz Biotechnology); anti- β -actin mouse mAb (AC15; Sigma); anti-HA rat mAb (3F10; Roche).

Cell culture and transfection

MDCK II cells were grown in Dulbecco's modified Eagle's medium (DMEM) supplemented with 10% fetal bovine serum (FBS), 100 U/ml penicillin and 100 U/ml streptomycin (Gibco-BRL) under a 5% CO₂ atmosphere and constant humidity. pEBV-

based stable transformants were established as described previously (Suzuki et al., 2004). Briefly, MDCK II cells (1×10^5 cells/cm²) were transfected with 3 μ g of pEB6-CAG or pOSTet14 expression vectors using Lipofectamine 2000 (Invitrogen) according to the manufacturer's instructions. The cells were reseeded on the following day at one-fifth of the cell density, and subjected to selection using DMEM containing 1.5 mg/ml geneticin (Gibco-BRL) for 6 hours after reseeding. To induce expression of the protein subcloned in pOSTet14, 20 or 200 ng/ml doxycycline was added to the culture medium. When cells were grown in 2D cultures they were seeded on Transwell filters (Corning Costar) at 3×10^5 cells/cm² and grown for 1-2 days to produce confluent monolayers. A CS was applied to well-polarized cells as described previously (Suzuki et al., 2001).

Three-dimensional culture

MDCK cell cyst formation was performed as described previously (O'Brien et al., 2001; Yamanaka et al., 2006). Briefly, MDCK II cells were trypsinized and suspended in ice-cold DMEM containing 2 μ g/ml calf skin type I collagen (Koken), 20 mM HEPES (pH 7.4) and 5% FBS. The resulting suspension was placed on Transwell filters. After formation of a gel at 37°C, growth medium was added to the wells. The cells were incubated for several days to allow cyst formation in the gel.

RNAi and rescue experiments

To establish pEB-based stable transformants expressing PAR-3 shRNAs, pEB-SUPER constructs expressing PAR-3-specific shRNAs were introduced into MDCK II cells and subjected to selection as described previously (Suzuki et al., 2004). The RNAi sequences used for canine PAR-3 were as follows: 1, 5'-CAUGGAGAU-GGAGGAUAC-3'; 2, 5'-GACAGACUGGUAGCAGUGU-3'; and 3, 5'-GAACA-GGATGAGGATGGGA-3' (Yamanaka et al., 2006). Canine PAR-6 β in MDCK cells was knocked down with the following RNAi sequences: 2, 5'-TGGAGACTTACT-ACCTATA-3'; and 5, 5'-GCACAGGACTATTAGCTGT-3'. The negative control RNAi sequence was described previously (Suzuki et al., 2004). The PAR-3 knockdown stable MDCK clones were also described previously (Yamanaka et al., 2006). Briefly, clone 13-32 stably expresses PAR-3 shRNA sequence 2, whereas clone 25a stably expresses PAR-3 shRNA sequences 1 and 3. The latter clone was used for rescue experiments with rat PAR-3. The corresponding negative control clones (11-10 and 1-5) were also described previously (Yamanaka et al., 2006).

Immunofluorescence and quantification of ZO-1 staining

MDCK cells were fixed with 2% paraformaldehyde, permeabilized with 0.5% Triton X-100 in PBS and stained after blocking with 10% calf serum in PBS (Suzuki et al., 2001). Cells cultured in collagen gels were processed in a similar manner except that the incubation time for each procedure was prolonged. The secondary antibodies used were Alexa Fluor 488- or 647-conjugated goat antibodies against rabbit, mouse or rat IgG (Molecular Probes) and Cy3-conjugated goat anti-rabbit antibodies (Amersham Bioscience). Rhodamine-phalloidin was used to visualize filamentous actin (Molecular Probes). Cell nuclei were stained with TOPRO3 (Invitrogen). Samples were mounted with PBS (pH 8.5) containing 50% (w/v) glycerol and 0.01% (w/v) *p*-phenylenediamine (Wako), and examined using a Zeiss LSM510 confocal microscope or a disc confocal system equipped with CSU10 (Yokogawa) and an Orca II CCD camera (Hamamatsu Photonics).

To quantify the average ZO-1 signal intensity per cell, three fields of MDCK cells were randomly selected from each sample, and the total intensity of ZO-1 staining in each field was measured using Multi Gauge software (Fujifilm). The cell numbers were counted in each field based on nuclear staining with 4',6-diamidino-2-phenylindole (DAPI), and the mean ZO-1 staining intensity per cell was calculated.

Electron microscopy

Cells cultured on filters were fixed with fresh 2% formaldehyde and 2.5% glutaraldehyde in 0.1 M phosphate buffer (pH 6.8) for 2 hours at room temperature and then postfixed with 1% OsO₄ in the same buffer for 2 hours on ice. Cells were rinsed with distilled water, stained with 0.5% aqueous uranyl acetate overnight at room temperature, dehydrated with ethanol and embedded in Polybed 812 (Polyscience). Ultrathin sections were cut with a diamond knife, double-stained with uranyl acetate and lead citrate, and examined with a JEM 1010 transmission electron microscope (JEOL) operated at an accelerating voltage of 100 kV.

For immunoelectron microscopy, cells cultured on plastic dishes were fixed and stained as described for immunofluorescent analysis, except that anti-rabbit IgG coupled with 5 nm gold (BBInternational) was used as a secondary antibody. Samples were then fixed with 1% glutaraldehyde in PBS overnight at 4°C, and then postfixed with 1% OsO₄ in 0.1 M phosphate buffer for 2 hours on ice. The samples were dehydrated with a graded series of ethanol, which were finally substituted with propylene oxide. The samples were then embedded in Epoxy resin.

We are deeply grateful to Natsuko Izumi for determining the efficient PAR-6 RNAi sequences in MDCK cells, Kazuyo Misaki for assistance with electron microscopy, and Shiro Suetsugu (Tokyo University, Japan) for helpful comments. This study was supported by grants from the Ministry of Education, Culture, Sports, Science and Technology of

Japan (S.O.) and the Japanese Society for the Promotion of Science (S.O. and A.S.), and by a Grant-in-Aid for Young Scientists Start-up (19870019).

References

- Aceto, D., Beers, M. and Kemphues, K. J. (2006). Interaction of PAR-6 with CDC-42 is required for maintenance but not establishment of PAR asymmetry in *C. elegans*. *Dev. Biol.* **299**, 386-397.
- Adachi, M., Inoko, A., Hata, M., Furuse, K., Umeda, K., Itoh, M. and Tsukita, S. (2006). Normal establishment of epithelial tight junctions in mice and cultured cells lacking expression of ZO-3, a tight-junction MAGUK protein. *Mol. Cell. Biol.* **26**, 9003-9015.
- Atwood, S. X., Chabu, C., Penkert, R. R., Doe, C. Q. and Prehoda, K. E. (2007). Cdc42 acts downstream of Bazooka to regulate neuroblast polarity through Par-6 aPKC. *J. Cell Sci.* **120**, 3200-3206.
- Bayless, K. J. and Davis, G. E. (2002). The Cdc42 and Rac1 GTPases are required for capillary lumen formation in three-dimensional extracellular matrices. *J. Cell Sci.* **115**, 1123-1136.
- Bilder, D., Schober, M. and Perrimon, N. (2003). Integrated activity of PDZ protein complexes regulates epithelial polarity. *Nat. Cell Biol.* **5**, 53-58.
- Chen, X. and Macara, I. G. (2005). Par-3 controls tight junction assembly through the Rac exchange factor Tiam1. *Nat. Cell Biol.* **7**, 262-269.
- Folkman, J. and Haudenschild, C. (1980). Angiogenesis *in vitro*. *Nature* **288**, 551-556.
- Harris, T. J. and Peifer, M. (2004). Adherens junction-dependent and -independent steps in the establishment of epithelial cell polarity in *Drosophila*. *J. Cell Biol.* **167**, 135-147.
- Harris, T. J. and Peifer, M. (2005). The positioning and segregation of apical cues during epithelial polarity establishment in *Drosophila*. *J. Cell Biol.* **170**, 813-823.
- Hirose, T., Izumi, Y., Nagashima, Y., Tamai-Nagai, Y., Kurihara, H., Sakai, T., Suzuki, Y., Yamanaka, T., Suzuki, A., Mizuno, K. et al. (2002). Involvement of ASIP/Par-3 in the promotion of epithelial tight junction formation. *J. Cell Sci.* **115**, 2485-2495.
- Hirose, T., Karasawa, M., Sugitani, Y., Fujisawa, M., Akimoto, K., Ohno, S. and Noda, T. (2006). PAR3 is essential for cyst-mediated epicardial development by establishing apical cortical domains. *Development* **133**, 1389-1398.
- Hurd, T. W., Fan, S., Liu, C. J., Kweon, H. K., Hakansson, K. and Margolis, B. (2003a). Phosphorylation-dependent binding of 14-3-3 to the polarity protein Par3 regulates cell polarity in mammalian epithelia. *Curr. Biol.* **13**, 2082-2090.
- Hurd, T. W., Gao, L., Roh, M. H., Macara, I. G. and Margolis, B. (2003b). Direct interaction of two polarity complexes implicated in epithelial tight junction assembly. *Nat. Cell Biol.* **5**, 137-142.
- Hutterer, A., Betschinger, J., Petronczki, M. and Knoblich, J. A. (2004). Sequential roles of Cdc42, Par-6, aPKC, and Lgl in the establishment of epithelial polarity during *Drosophila* embryogenesis. *Dev. Cell* **6**, 845-854.
- Izumi, Y., Hirose, T., Tamai, Y., Hirai, S., Nagashima, Y., Fujimoto, T., Tabuse, Y., Kemphues, K. J. and Ohno, S. (1998). An atypical PKC directly associates and colocalizes at the epithelial tight junction with ASIP, a mammalian homologue of *Caenorhabditis elegans* polarity protein PAR-3. *J. Cell Biol.* **143**, 95-106.
- Kamei, M., Saunders, W. B., Bayless, K. J., Dye, L., Davis, G. E. and Weinstein, B. M. (2006). Endothelial tubes assemble from intracellular vacuoles *in vivo*. *Nature* **442**, 453-456.
- Knust, E. and Bossinger, O. (2002). Composition and formation of intercellular junctions in epithelial cells. *Science* **298**, 1955-1959.
- Lakkaraju, A. and Rodriguez-Boulton, E. (2007). Cell biology: caught in the traffic. *Nature* **448**, 266-267.
- Lin, D., Edwards, A. S., Fawcett, J. P., Mbamalu, G., Scott, J. D. and Pawson, T. (2000). A mammalian PAR-3-PAR-6 complex implicated in Cdc42/Rac1 and aPKC signalling and cell polarity. *Nat. Cell Biol.* **2**, 540-547.
- Louvard, D. (1980). Apical membrane aminopeptidase appears at site of cell-cell contact in cultured kidney epithelial cells. *Proc. Natl. Acad. Sci. USA* **77**, 4132-4136.
- Macara, I. G. (2004). Parsing the polarity code. *Nat. Rev. Mol. Cell Biol.* **5**, 220-231.
- Martin-Belmonte, F., Gassama, A., Datta, A., Yu, W., Rescher, U., Gerke, V. and Mostov, K. (2007). PTEN-mediated apical segregation of phosphoinositides controls epithelial morphogenesis through Cdc42. *Cell* **128**, 383-397.
- Mishima, A., Suzuki, A., Enaka, M., Hirose, T., Mizuno, K., Ohnishi, T., Mohri, H., Ishigatsubo, Y. and Ohno, S. (2002). Over-expression of PAR-3 suppresses contact-mediated inhibition of cell migration in MDCK cells. *Genes Cells* **7**, 581-596.
- Mishima, W., Suzuki, A., Yamaji, S., Yoshimi, R., Ueda, A., Kaneko, T., Tanaka, J., Miwa, Y., Ohno, S. and Ishigatsubo, Y. (2004). The first CH domain of afillin activates Cdc42 and Rac1 through alphaPIX, a Cdc42/Rac1-specific guanine nucleotide exchanging factor. *Genes Cells* **9**, 193-204.
- Mizuno, K., Suzuki, A., Hirose, T., Kitamura, K., Kutsuzawa, K., Futaki, M., Amano, Y. and Ohno, S. (2003). Self-association of PAR-3-mediated by the conserved N-terminal domain contributes to the development of epithelial tight junctions. *J. Biol. Chem.* **278**, 31240-31250.
- Mostov, K. and Martin-Belmonte, F. (2006). Developmental biology: the hole picture. *Nature* **442**, 363-364.
- Mostov, K., Su, T. and ter Beest, M. (2003). Polarized epithelial membrane traffic: conservation and plasticity. *Nat. Cell Biol.* **5**, 287-293.
- Nagai-Tamai, Y., Mizuno, K., Hirose, T., Suzuki, A. and Ohno, S. (2002). Regulated protein-protein interaction between aPKC and PAR-3 plays an essential role in the polarization of epithelial cells. *Genes Cells* **7**, 1161-1171.
- Nakayama, M., Goto, T. M., Sugimoto, M., Nishimura, T., Shinagawa, T., Ohno, S., Amano, M. and Kaibuchi, K. (2008). Rho-kinase phosphorylates PAR-3 and disrupts PAR complex formation. *Dev. Cell* **14**, 205-215.
- Nam, S. C. and Choi, K. W. (2003). Interaction of Par-6 and Crumbs complexes is essential for photoreceptor morphogenesis in *Drosophila*. *Development* **130**, 4363-4372.
- Nishimura, T., Kato, K., Yamaguchi, T., Fukata, Y., Ohno, S. and Kaibuchi, K. (2004). Role of the PAR-3-KIF3 complex in the establishment of neuronal polarity. *Nat. Cell Biol.* **6**, 328-334.
- Nishimura, T., Yamaguchi, T., Kato, K., Yoshizawa, M., Nabeshima, Y., Ohno, S., Hoshino, M. and Kaibuchi, K. (2005). PAR-6-PAR-3 mediates Cdc42-induced Rac activation through the Rac GEFs STEF/Tiam1. *Nat. Cell Biol.* **7**, 270-277.
- O'Brien, L. E., Jou, T. S., Pollack, A. L., Zhang, Q., Hansen, S. H., Yurchenco, P. and Mostov, K. E. (2001). Rac1 orientates epithelial apical polarity through effects on basolateral laminin assembly. *Nat. Cell Biol.* **3**, 831-838.
- O'Brien, L. E., Zegers, M. M. and Mostov, K. E. (2002). Opinion: building epithelial architecture: insights from three-dimensional culture models. *Nat. Rev. Mol. Cell Biol.* **3**, 531-537.
- Straight, S. W., Shin, K., Fogg, V. C., Fan, S., Liu, C. J., Roh, M. and Margolis, B. (2004). Loss of PALSL1 expression leads to tight junction and polarity defects. *Mol. Biol. Cell* **15**, 1981-1990.
- Suzuki, A. and Ohno, S. (2006). The PAR-aPKC system: lessons in polarity. *J. Cell Sci.* **119**, 979-987.
- Suzuki, A., Yamanaka, T., Hirose, T., Manabe, N., Mizuno, K., Shimizu, M., Akimoto, K., Izumi, Y., Ohnishi, T. and Ohno, S. (2001). Atypical protein kinase C is involved in the evolutionarily conserved par protein complex and plays a critical role in establishing epithelia-specific junctional structures. *J. Cell Biol.* **152**, 1183-1196.
- Suzuki, A., Ishiyama, C., Hashiba, K., Shimizu, M., Ebnet, K. and Ohno, S. (2002). aPKC kinase activity is required for the asymmetric differentiation of the premature junctional complex during epithelial cell polarization. *J. Cell Sci.* **115**, 3565-3573.
- Suzuki, A., Hirata, M., Kamimura, K., Maniwa, R., Yamanaka, T., Mizuno, K., Kishikawa, M., Hirose, H., Amano, Y., Izumi, N. et al. (2004). aPKC acts upstream of PAR-1b in both the establishment and maintenance of mammalian epithelial polarity. *Curr. Biol.* **14**, 1425-1435.
- Tanentzapf, G. and Tepass, U. (2003). Interactions between the crumbs, lethal giant larvae and bazooka pathways in epithelial polarization. *Nat. Cell Biol.* **5**, 46-52.
- Vega-Salas, D. E., Salas, P. J. and Rodriguez-Boulton, E. (1987). Modulation of the expression of an apical plasma membrane protein of Madin-Darby canine kidney epithelial cells: cell-cell interactions control the appearance of a novel intracellular storage compartment. *J. Cell Biol.* **104**, 1249-1259.
- Vega-Salas, D. E., Salas, P. J. and Rodriguez-Boulton, E. (1988). Exocytosis of vacuolar apical compartment (VAC): a cell-cell contact controlled mechanism for the establishment of the apical plasma membrane domain in epithelial cells. *J. Cell Biol.* **107**, 1717-1728.
- Vogelmann, R. and Nelson, W. J. (2005). Fractionation of the epithelial apical junctional complex: reassessment of protein distributions in different substructures. *Mol. Biol. Cell* **16**, 701-716.
- Wu, H., Feng, W., Chen, J., Chan, L. N., Huang, S. and Zhang, M. (2007). PDZ domains of Par-3 as potential phosphoinositide signaling integrators. *Mol. Cell* **28**, 886-898.
- Yamanaka, T., Horikoshi, Y., Suzuki, A., Sugiyama, Y., Kitamura, K., Maniwa, R., Nagai, Y., Yamashita, A., Hirose, T., Ishikawa, H. et al. (2001). PAR-6 regulates aPKC activity in a novel way and mediates cell-cell contact-induced formation of the epithelial junctional complex. *Genes Cells* **6**, 721-731.
- Yamanaka, T., Horikoshi, Y., Sugiyama, Y., Ishiyama, C., Suzuki, A., Hirose, T., Iwamatsu, A., Shinohara, A. and Ohno, S. (2003). Mammalian Lgl forms a protein complex with PAR-6 and aPKC independently of PAR-3 to regulate epithelial cell polarity. *Curr. Biol.* **13**, 734-743.
- Yamanaka, T., Horikoshi, Y., Izumi, N., Suzuki, A., Mizuno, K. and Ohno, S. (2006). Lgl mediates apical domain disassembly by suppressing the PAR-3-aPKC-PAR-6 complex to orient apical membrane polarity. *J. Cell Sci.* **119**, 2107-2118.
- Yeaman, C., Grindstaff, K. K. and Nelson, W. J. (1999). New perspectives on mechanisms involved in generating epithelial cell polarity. *Physiol. Rev.* **79**, 73-98.